Title

Improving the Accuracy of Modelling CO2 Electroreduction on Copper Using Many-Body Perturbation Theory

Journal

Angewandte Chemie International Edition, 61(43)

ISSN

1433-7851

Authors

Wei, Ziyang
Sautet, Philippe

Publication Date

2022-10-24

DOI

10.1002/anie.202210060

Improving the Accuracy of Modelling CO_2 Electroreduction on Copper Using Many-Body Perturbation Theory

Ziyang Wei[1] Philippe Sautet*,[1,2]
sautet@ucla.edu

[1] Department of Chemistry and Biochemistry, University of California, Los Angeles, California, 90095, United States
[2] Department of Chemical and Biomolecular Engineering, University of California, Los Angeles, California, 90095, United States

Abstract

Copper (Cu) remains the most important metal catalyst for the carbon dioxide reduction reaction (CO_2RR) into C_2 products. Due to limited evidence from *in situ* experiments, mechanistic studies are often performed in the framework of density functional theory (DFT), using functionals at the generalized gradient approximation (GGA) level, which have fundamental difficulties to correctly describe CO adsorption and surface stability. We employ the adiabatic connection fluctuation dissipation theorem within the random phase approximation (RPA), in combination with the linearized Poisson-Boltzmann equation to describe solvation effects, to investigate the mechanism of CO_2RR on the Cu(100) facet. Qualitatively different from the DFT-GGA results, RPA results propose the formation of *OCCHO as the potential determining step towards C2 products. The results suggest that it is important to use more accurate methods like RPA when modeling reactions involving multiple CO-related species like CO_2RR.

The electrochemical carbon dioxide reduction reaction (CO_2RR) has attracted tremendous interest[1–3] since its discovery by Hori et al[4]. After years, Cu remains the most important metal catalyst towards C_2 products[5,6], including ethylene and ethanol, while other metal catalysts mainly produce formate (Pb, In, and Sn) or CO (Au, Ag, Zn, and Pd)[4]. Specifically, the Cu(100) facet has been reported to selectively produce C_2 products at low overpotentials[5]. Although tremendous efforts have been devoted to elucidating the reaction mechanism, the detailed reaction pathways, and especially the nature of the potential-determining step (PDS) are controversial from the experimental side due to limited *in situ* spectroscopy. Computational studies based on density functional theory (DFT) energetics have also been conducted to clarify the reaction mechanism but the conclusion is under debate as well. Regarding the critical C-C coupling step, Calle-Vallejo et al.[7] used the Perdew-Burke-Ernzerhof (PBE) functional[8] and concluded that the PDS is the hydrogenation of *OCCO to form *OCCOH, preceded by an OC-CO coupling. Montoya et al.[9] used the revised Perdew-Burke-Ernzerhof (RPBE) functional[10] with a charged explicit solvating water layer and concluded the OC-CO coupling to give *OCCO with a different structure compared to the one proposed by Calle-Vallejo et al.[7]. Peng et al.[11] used the Bayesian error estimation functional[12] (BEEF) and found the step from *OCCO to *OCCOH to be potential limiting at low overpotential and C-CO coupling to be favored at high overpotential. Regarding other facets, Liu et al.[13] used BEEF and also found the OC-CO coupling followed by hydrogenation to *OCCOH to be favored on Cu(211). Hussain et al.[14] used the RPBE functional and found ethylene is formed by coupling two $*CH_2$ fragments on Cu(111).

Nevertheless, the aforementioned theoretical studies utilized exchange correlation (XC) functionals at the generalized-gradient approximation (GGA) level while it is difficult for such semi-local density functionals to give simultaneously correct CO adsorption energies and surface energies for Cu(111)[15] and (100) facets[16]. Functionals which describe CO adsorption strength accurately such as RPBE give surface energies[16] underestimated by over 0.5 J/m^2 (ca. 30% of experimental value as 1.8 J/m^2). In addition, all the semi-local functionals fail to predict the correct site for CO adsorption on both Cu(100) and Cu(111) facets, which is often referred to as the CO-adsorption puzzle[17]. These fundamental deficiencies of semi-local density functionals to describe CO adsorption and surface stability naturally raise the question regarding the accuracy of

GGA functionals for the intermediate species involved in CO_2RR. This is especially crucial since conclusions on catalytic activity are often derived from the computed results that initial hydrogenation[18] and/or C-C coupling steps[7,9,19], involving formation of species as *COH, *CHO, *OCCO, *OCCOH, and *OCCHO, are the PDSs. Despite the chemical importance of the mechanistic conclusions taken using DFT-GGA calculations, there is no assessment, to our knowledge, of the accuracy of these exchange-correlation functionals for the CO_2 electrocatalytic reduction on the Cu(100) facet.

Therefore, to correctly describe the CO_2RR process, a method addressing all of the aforementioned issues is necessary. *Ad hoc* corrections[20,21] do not serve the purpose as the values needed for the intermediates other than CO are generally unknown. Here we propose to consider the adiabatic connection fluctuation dissipation theorem[22,23] (ACFDT) within the random phase approximation[24,25] (RPA), which has been shown to simultaneously correctly describe the Cu(100) surface energy and the CO adsorption on Cu(100)[16]. It is worth noting that the density functional embedding theorem (DFET) developed by Carter et al.[26] has achieved considerable success in describing both the CO adsorption[27] and recently the hydrogenation steps in CO_2RR[28]. The RPA method avoids the symmetry mismatch between the embedded cluster and the metallic surface faced in DFET, benefitting from the fact that an implementation for plane waves in periodic boundary conditions exists. Moreover, the implementation in periodic boundary conditions also gives great convenience to incorporate the existing implicit solvation models, while a explicit solvation description using high level methods requires excessive amount of resources and is hence not affordable. Here we show that it is natural and convenient to incorporate the implicit solvation effects, more specifically, by combining the linearized Poisson-Boltzmann (lPB) equation[29,30] into the RPA frame. We apply this method to the CO_2RR on the Cu(100) facet, focusing on the CO hydrogenation and C-C coupling steps.

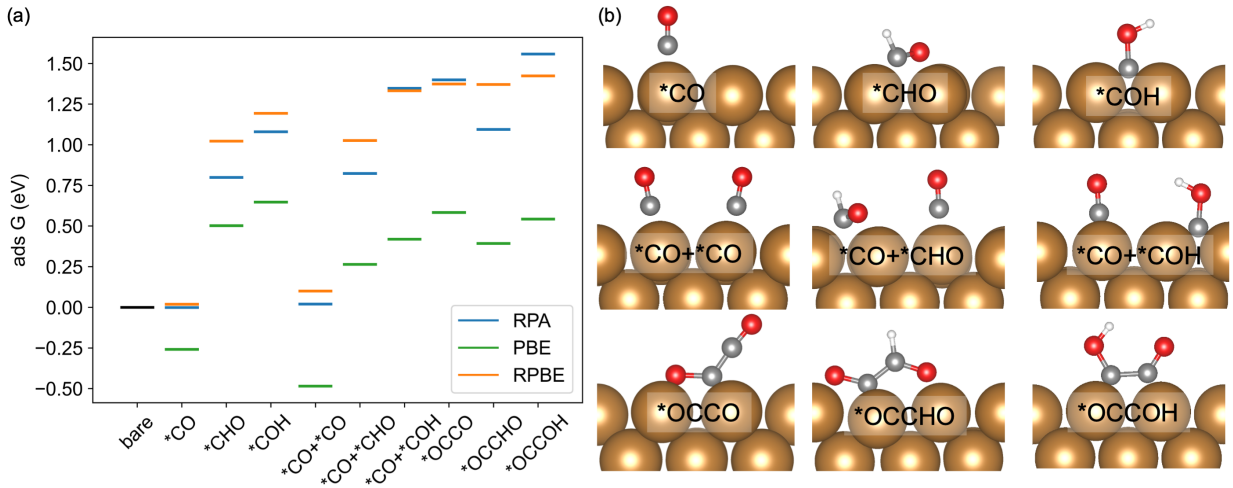

Figure 1: (a) Energetics of CO_2RR intermediates considered, *CO, *CHO, *COH, *CO+*CO, *CO+*CHO, *CO+*COH, *OCCO, *OCCHO, and *OCCOH, using RPA and PBE/RPBE functionals at the Cu(100)-vacuum interface. (b) Side view of the atomic structures. For adsorbates with multiple possible sites, energetics are considered for the one with the most stable RPA energy. Cu atoms are shown as brown, O atoms red, C atoms grey, and H atoms white.

Fig. 1 shows the RPA energetics of the considered intermediate species, *CO, *CHO, *COH, *CO+*CO, *CO+*CHO, *CO+*COH, *OCCO, *OCCHO, and *OCCOH, in comparison with PBE/RPBE energetics at the Cu(100)-vacuum interface. The energetics are presented following the computational hydrogen electrode (CHE) framework[31], with a potential of 0 V vs RHE. The PBE energetics show a severe overbinding by 0.25 to 0.5 eV per CO component, in line with the reported overestimation of the CO adsorption strength.[15,16] In the work of Calle-Vallejo et al.[7], a 0.24 eV correction per CO was applied and this turns to be generally working for *CO, *CO+*CO, and *CHO. However, for all the *COH related adsorbates and coupled adsorbates including *OCCO, *OCCHO, and *OCCOH, this correction appears to be still markedly insufficient. On the other hand, the RPBE energetics show a significant underbinding for most intermediates,

consistent with the underestimated Cu(100) surface energy. It is worth mentioning that for the co-adsorption structures, *CO+*CO and *CO+*CHO, we found the top site CO to be more stable than bridge site CO, in contrast to the PBE prediction due to the known site error (CO puzzle). For the case of *CO+*COH, the top site minimum is not locally stable and was optimized to bridge site CO using DFT methods and we just use this structure. We leave the discussion of detailed energetics to the next paragraph after solvation effects are considered.

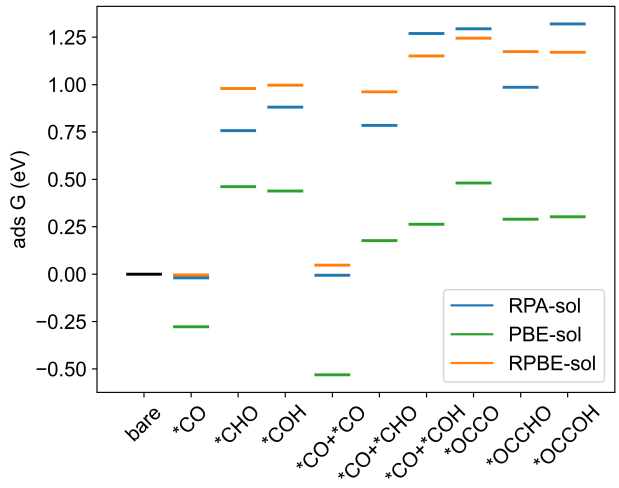

Figure 2: Implicitly solvated energetics of CO_2RR intermediates considered, *CO, *CHO, *COH, *CO+*CO, *CO+*CHO, *CO+*COH, *OCCO, *OCCHO, and *OCCOH, using RPA and PBE/RPBE functionals on Cu(100). The methods are termed as -sol to be distinguished from the vacuum energetics.

The water solvation effects are critical for the CO_2RR while the explicit solvation is rather computationally expensive and hence beyond our current computational capability at the RPA level. Therefore, we combine the implicit solvation method, more specifically, the implementation of the lPB equation by Hennig et al.[29,30], into the RPA frame, named as RPA-sol (see the Supporting Information (SI) section 2). The RPA-sol energetics are shown in Fig. 2, in comparison with implicitly solvated PBE-sol and RPBE-sol energetics. While PBE-sol and RPBE-sol predict similar stability for hydrogenated *CHO and *COH species, RPA-sol predicts *CHO to be 0.12 eV more stable, in line with the results on Cu(111) using DFET[28]. A similar yet more significant phenomenon is observed for the coupling intermediates, *OCCHO and *OCCOH: RPA-sol energetics show that *OCCHO is stabilized by 0.34 eV compared to *OCCOH, while RPBE-sol and PBE-sol show similar stability for these two intermediates. We have also tested the influence of van der Waals (vdW) corrections and found that the conclusion here is not sensitive to the vdW correction applied, as shown in the SI section 4.

The implicit solvation can be further improved as the lPB equation does not directly account for the directional hydrogen bonds. Therefore, as shown in the SI section 5, we compare different existing explicit solvation treatments[11,13,32–34], and some studies[11,13,14,34] found that the solvation energies of *OCCOH and *OCCHO are close. Among all the treatments considered, the treatment of Calle-Vallejo et al.[7] relatively stabilizes *OCCOH the most, with a stabilization of 0.38 eV for the COH part in *OCCOH and 0.10 eV for the CHO part in *OCCHO. Using this treatment, corresponding to an extra 0.16 eV stabilization for *OCCOH compared to *OCCHO on implicit solvation energetics, RPBE and PBE both predict *OCCOH to be more stable while RPA still predicts *OCCHO to be more stable by 0.18 eV, leading to the PDS changing from the formation of *OCCOH with RPBE or PBE to the formation of *OCCHO with RPA.

Adsorbate-adsorbate interactions can potentially play a role, and we have performed test calculations to evaluate them (SI section 7). We found the effect of adsorbate-adsorbate interactions on adsorption energies on the Cu(100) surface to be small when the CO coverage is below 0.5 ML, which is the highest coverage found from experiments[35] or kinetic modeling[13]. Hence, adsorbate-adsorbate interaction can be neglected in the current study. We have also considered the energetics of the further hydrogenation products along

the C_1 pathway, *CHOH and *CH_3, as shown in the SI section 8, and no qualitative difference was found between RPA energetics and GGA DFT energetics. Based on this finding and the conclusion of previous studies[7,9,36], we do not focus on further hydrogenation products along the C_1 pathway.

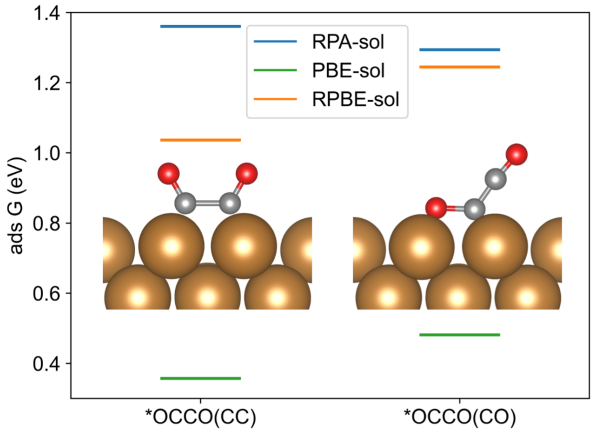

Figure 3: Implicitly solvated energetics of the *OCCO intermediate, considered for both the structure proposed by Calle-Vallejo et al.[7], *OCCO(CO) (right) and the structure proposed by Montoya et al.[9], *OCCO(CC) (left), using RPA and PBE/RPBE functionals. Side view of the atomic structures is presented as well, with Cu atoms shown as brown, O atoms red, C atoms grey, and H atoms white.

Among the C-C coupling intermediates, the *OCCO intermediate is involved in different mechanisms proposed using DFT energetics while being specifically controversial: Calle-Vallejo et al.[7] proposed a *OCCO structure binding with the Cu surface using one C atom and one O atom (denoted as *OCCO(CO) hereinafter), whereas Montoya et al.[9] found that an electric field or a charged water layer can stabilize the *OCCO binding with two C atoms (denoted as *OCCO(CC) hereinafter). Later Goodpaster et al.[37] reported that the *OCCO(CC) structure can also be obtained by charging the system, i.e., using a grand-canonical DFT treatment with implicit solvation. Essentially all these treatments apply extra electron density to stabilize the *OCCO(CC) intermediate. Here we investigate the energetics of both structures and results are shown in Fig. 3. The *OCCO(CC) structure is obtained by charging the surface using PBE-sol and RPBE-sol, respectively, while the reported energetics correspond to the single point energy calculated at neutral number of electrons. Interestingly, we find that RPBE-sol and PBE-sol show a significant stabilization of the *OCCO(CC) structure, 0.21 eV and 0.12 eV, respectively; RPA-sol, on the other hand, predicts the *OCCO(CO) structure to be 0.07 eV more stable. More importantly, the over-stabilization of *OCCO(CC) using GGA energetics casts doubt on the proposed mechanism involving formation of *OCCO(CC) by *CO coupling[9].

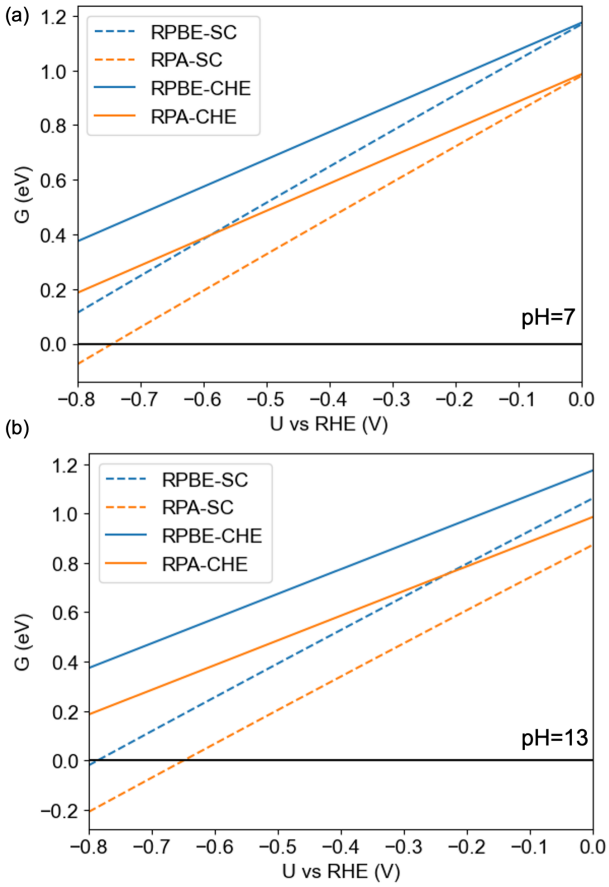

Figure 4: Potential dependent adsorption free energy of *OCCHO and predicted onset potential of ethylene production, using RPA and RPBE energetics, at condition of (a) pH=7 and (b) pH=13. The potential effects are treated at both the CHE and the SC level, with RPA-SC energetics being extrapolated as described in Eq. 1. The crossing point with the horizontal black line indicates the onset potential.

To validate the RPA energetics, we first consider the predicted onset potential of methane production using these RPA energetics. The predicted value (-0.76 V) matches well with the experimental value (-0.8 V), and better than the calculated RPBE value (-0.98 V) (see SI Fig. S7). We then move to the predicted onset potential for ethylene formation considering different coupling species as the PDS. Here, the RPA-sol energetics with CHE treatment, as shown in Fig. 2, suggest the formation of *OCCHO to be the PDS, whereas the predicted onset potential, -0.98 V, appears to be too negative compared to the experimental value[5], -0.4 V. The predicted onset potential using RPBE-sol is even more negative. We found a considerable amount of mismatch originating from the CHE treatment, as it lacks the description of the surface capacitance and the potential of zero charge. Therefore, we turn to the grand-canonical DFT treatment, namely, the surface charging (SC) method[30,38,39], which correctly accounts for these effects. The fully grand canonical treatment at the RPA level, namely RPA-SC, has been developed very recently[40] but requires extra computational cost and is not affordable for this system. Therefore, in this work, we present the extrapolated RPA-SC energetics using RPA-CHE, RPBE-SC, and RPBE-CHE energetics, as the RPBE-sol energetics are more similar to RPA-sol ones than PBE-sol ones:

$$G^{RPA-SC}_{extrapolated}(U) = G^{RPA-CHE}(U) + G^{RPBE-SC}(U) - G^{RPBE-CHE}(U) \quad (1)$$

As shown in Fig. 4, at the RPBE level, the onset potential of ethylene production changes significantly from $U^{RPBE-CHE}_{onset} = -1.17V$ to $U^{RPBE-SC}_{onset} - 0.88V$. The calculated capacitance and potential of zero charge values using the RPBE functional are provided in the SI table S12, and match well with the experimental

values. After applying this correction to RPA energetics, we get $U_{onset}^{RPA-SC,extrapolated} = -0.74V$, which is significantly lower than $U_{onset}^{RPA-CHE} = -0.98V$ and matches closer with the experimental value, -0.4 V at the condition of pH=7. The difference between the CHE and SC approaches for *OCCHO (0.24 V) is significantly larger than the difference for *CHO (0.01 V, see SI Fig. S7) due to the larger surface dipole moment of *OCCHO. The difference between $U_{onset}^{RPA-SC,extrapolated}$ and $U_{onset}^{RPBE-SC}$, 0.14 V, is not simply the difference between $U_{onset}^{RPA-CHE}$ and $U_{onset}^{RPBE-CHE}$, 0.19 V: in the SC treatment, the surface capacitance is determined *ab initio*, leading to a non-zero quadratic term in the calculated G-U relationship. This term also naturally predicts correctly the pH dependence of the onset potential: the RPA onset potential changes from $U_{onset}^{RPA-SC,extrapolated} = -0.74V$ to $U_{onset}^{RPA-SC,extrapolated} = -0.65V$ when pH is changed from 7 to 13, matching well with the experimental shift of 0.1 V.

Two reasons could be advocated to explain the remaining difference between the experimental (-0.4 V) and RPA predicted (-0.74 V) onset potential. The first one is linked with inaccuracies in the theoretical treatment and especially in the implicit description of solvation. A correction for explicit solvation effects can be added: if the solvation correction of Liu et al.[13], obtained from explicit static calculations, is applied, an onset potential of -0.45 V is obtained, matching very well with the experimental value of -0.4 V. The match of onset potential is hence comparable with the value for the *OCCOH pathway, OC-CO coupling followed by hydrogenation, achieved by Calle-Vallejo et al.[7] with PBE energetics, -0.4 V for Cu(100). It is worth mentioning that, considering the dynamic water structure with molecular dynamic simulations, Heenen et al.[33] found that the solvation is considerably weaker than that of the static water treatment considered in most publications, which indicates that the implicit solvation strength may be effectively close to the more realistic dynamic explicit solvation. Considering the recent experimental observation that a clean and defect-free Cu(100) surface has low CO_2RR activity[41], another reason could be that the RPA-SC onset potential correctly describes the intrinsic activity of Cu(100) and that the less negative experimental onset potential is related with the presence of defects and steps[41] on the catalysts. The RPA energetics of CO_2RR on defected or stepped surfaces is intriguing and is expected to be explored in the future.

We have further checked the predicted onset potential for ethylene, assuming formation of *OCCO (CC), *OCCO (CO), and *OCCOH as the PDS and extrapolated RPA onset potentials are found to be more negative than in the case of *OCCHO (SI section 9). Therefore, we conclude that the formation of *OCCHO is the PDS. Experimentally, Hori et al.[42] and Koper et al.[5] have shown that the pH dependence is different for C_1 and C_2 pathways. Koper's analysis[43] shows that the pH dependence of the CO_2RR on the RHE scale[44] suggests that the rate determining step does not involve a proton transfer or coupling of H containing adsorbates. Considering this, the formation of *OCCHO may result from coupling of two *CO species followed by a proton-electron transfer to form *OCCHO. This mechanism differs from the DFT mechanism proposed by Calle-Vallejo et al.[7] by the nature of the hydrogenation product (*OCCHO with RPA compared to *OCCOH with GGA-DFT) due to the DFT underbinding of CHO related species. Moreover, using *in situ* Fourier transform infrared spectroscopy, Koper et al.[45] observed vibrational frequencies of 1191 cm^{-1} and 1584 cm^{-1} and found the vibrational frequencies of *OCCOH to be compatible. We found that *OCCHO gives an IR active mode at 1194 cm^{-1} and that *OCCHOH, the further hydrogenation product of *OCCHO, provides an IR active mode at 1534 cm^{-1}, indicating that the *OCCHO pathway can also be compatible with the experimental observations (see SI for the vibrational modes). Moreover, we would like to note that the current treatment assumes that the kinetics are in line with the thermodynamics. A more comprehensive approach requires to calculate the reaction barriers and can be combined with micro-kinetic modeling, allowing better comparison with experimental results[11,13,14], including the selectivity among hydrogen evolution reaction, C_1 products and C_2 products. However, the atomic forces at the RPA level for periodic slab systems are beyond our current computational power and these aspects may be included in the future. The description of cation and halide effects at the RPA level is also intriguing while a detailed analysis goes beyond the scope of this work.

To summarize, our results clearly show qualitative and quantitative differences between the more accurate RPA energetics and the PBE/RPBE results, as well as the previous studies using the semi-local density functionals. Formation of *OCCHO is proposed as the PDS, yielding onset potential matching well with experimental value and satisfying the observation that the rate determining step does not involve a proton. The shortcomings of the semi-local XC functionals suggest that interpretation based on DFT energetics may need to be more cautious, and it is important to consider the difference between these functionals and more accurate methods like RPA or DFET, when modeling CO_2RR which involves adsorption across various

species. The results also suggest that the modeling of defective and stepped surfaces may be essential to understand the observed activity of Cu catalysts for C-C formation.

Acknowledgement

This work is supported by the National Science Foundation under grant 2103116. The calculations were performed on the Hoffman2 cluster at UCLA Institute for Digital Research and Education (IDRE) and the Extreme Science and Engineering Discovery Environment (XSEDE)[46], which is supported by National Science Foundation grant number ACI-1548562, through allocation TG-CHE170060.

References

[1] S. Nitopi, E. Bertheussen, S. B. Scott, X. Liu, A. K. Engstfeld, S. Horch, B. Seger, I. E. Stephens, K. Chan, C. Hahn, J. K. Nørskov, T. F. Jaramillo, I. Chorkendorff, *Chem. Rev.* **2019**, *119*, 7610–7672.

[2] Y. Hori in *Modern Aspects of Electrochemistry*, Springer New York, **2008**, pp. 89–189.

[3] M. G. Kibria, J. P. Edwards, C. M. Gabardo, C. Dinh, A. Seifitokaldani, D. Sinton, E. H. Sargent, *Adv. Mater.* **2019**, *31*, 1807166.

[4] Y. Hori, K. Kikuchi, S. Suzuki, *Chem. Lett.* **1985**, *14*, 1695–1698.

[5] K. J. P. Schouten, Z. Qin, E. Pérez Gallent, M. T. Koper, *J. Am. Chem. Soc.* **2012**, *134*, 9864–9867.

[6] Y. Hori, I. Takahashi, O. Koga, N. Hoshi, *J. Phys. Chem. B* **2001**, *106*, 15–17.

[7] F. Calle-Vallejo, M. T. Koper, *Angew. Chem. Int. Ed.* **2013**, *52*, 7282–7285.

[8] J. P. Perdew, K. Burke, M. Ernzerhof, *Phys. Rev. Lett.* **1996**, *77*, 3865–3868.

[9] J. H. Montoya, C. Shi, K. Chan, J. K. Nørskov, *J. Phys. Chem. Lett.* **2015**, *6*, 2032–2037.

[10] B. Hammer, L. Hansen, J. Nørskov, *Phys. Rev. B* **1999**, *59*, 7413–7421.

[11] H. Peng, M. T. Tang, X. Liu, P. Schlexer Lamoureux, M. Bajdich, F. Abild-Pedersen, *Energy Environ. Sci.* **2021**, *14*, 473–482.

[12] J. Wellendorff, K. T. Lundgaard, A. Møgelhøj, V. Petzold, D. D. Landis, J. K. Nørskov, T. Bligaard, K. W. Jacobsen, *Phys. Rev. B* **2012**, *85*, 235149.

[13] X. Liu, P. Schlexer, J. Xiao, Y. Ji, L. Wang, R. B. Sandberg, M. Tang, K. S. Brown, H. Peng, S. Ringe, C. Hahn, T. F. Jaramillo, J. K. Nørskov, K. Chan, *Nat. Commun.* **2019**, *10*, 32.

[14] J. Hussain, H. Jónsson, E. Skúlason, *ACS Catal.* **2018**, *8*, 5240–5249.

[15] L. Schimka, J. Harl, A. Stroppa, A. Grüneis, M. Marsman, F. Mittendorfer, G. Kresse, *Nat. Mater.* **2010**, *9*, 741–744.

[16] Z. Wei, F. Göltl, P. Sautet, *J. Chem. Theory Comput.* **2021**, *17*, 7862–7872.

[17] P. J. Feibelman, B. Hammer, J. Nørskov, F. Wagner, M. Scheffler, R. Stumpf, R. Watwe, J. Dumesic, *J. Phys. Chem. B* **2000**, *105*, 4018–4025.

[18] A. J. Garza, A. T. Bell, M. Head-Gordon, *ACS Catal.* **2018**, *8*, 1490–1499.

[19] T. Cheng, H. Xiao, W. A. Goddard, *Proc. Natl. Acad. Sci. U.S.A.* **2017**, *114*, 1795–1800.

[20] S. E. Mason, I. Grinberg, A. M. Rappe, *Phys. Rev. B* **2004**, *69*, 161401.

[21] M. Gajdoš, J. Hafner, *Surf. Sci.* **2005**, *590*, 117–126.

[22] O. Gunnarsson, B. Lundqvist, *Phys. Rev. B* **1976**, *13*, 4274–4298.

[23] D. C. Langreth, J. P. Perdew, *Phys. Rev. B* **1977**, *15*, 2884–2901.

[24] P. Nozières, D. Pines, *Phys. Rev.* **1958**, *111*, 442–454.

[25] J. Harl, G. Kresse, *Phys. Rev. B* **2008**, *77*, 045136.

[26] C. Huang, M. Pavone, E. A. Carter, *J. Chem. Phys.* **2011**, *134*, 154110.

[27] S. Sharifzadeh, P. Huang, E. Carter, *J. Phys. Chem. C* **2008**, *112*, 4649–4657.

[28] Q. Zhao, J. M. P. Martirez, E. A. Carter, *J. Am. Chem. Soc.* **2021**, *143*, 6152–6164.

[29] K. Mathew, R. Sundararaman, K. Letchworth-Weaver, T. Arias, R. G. Hennig, *J. Chem. Phys.* **2014**, *140*, 084106.

[30] K. Mathew, V. C. Kolluru, S. Mula, S. N. Steinmann, R. G. Hennig, *J. Chem. Phys.* **2019**, *151*, 234101.

[31] J. Nørskov, J. Rossmeisl, A. Logadottir, L. Lindqvist, J. Kitchin, T. Bligaard, H. Jónsson, *J. Phys. Chem. B* **2004**, *108*, 17886–17892.

[32] T. Ludwig, J. A. Gauthier, C. F. Dickens, K. S. Brown, S. Ringe, K. Chan, J. K. Nørskov, *J. Phys. Chem. C* **2020**, *124*, 24765–24775.

[33] H. H. Heenen, J. A. Gauthier, H. H. Kristoffersen, T. Ludwig, K. Chan, *J. Chem. Phys.* **2020**, *152*, 144703.

[34] T. Ludwig, J. A. Gauthier, K. S. Brown, S. Ringe, J. K. Nørskov, K. Chan, *J. Phys. Chem. C* **2019**, *123*, 5999–6009.

[35] J. H. Baricuatro, Y.-G. Kim, C. L. Korzeniewski, M. P. Soriaga, *Electrochem. Commun.* **2018**, *91*, 1–4.

[36] J. H. Montoya, A. A. Peterson, J. K. Nørskov, *ChemCatChem* **2013**, *5*, 737–742.

[37] J. D. Goodpaster, A. T. Bell, M. Head-Gordon, *J. Phys. Chem. Lett.* **2016**, *7*, 1471–1477.

[38] S. N. Steinmann, C. Michel, R. Schwiedernoch, P. Sautet, *Phys. Chem. Chem. Phys.* **2015**, *17*, 13949–13963.

[39] S. N. Steinmann, P. Sautet, *J. Phys. Chem. C* **2016**, *120*, 5619–5623.

[40] Z. Wei, F. Göltl, S. N. Steinmann, P. Sautet, *J. Phys. Chem. Lett.* **2022**, 6079–6084.

[41] F. Scholten, K.-L. C. Nguyen, J. P. Bruce, M. Heyde, B. Roldan Cuenya, *Angew. Chem. Int. Ed.* **2021**, *60*, 19169–19175.

[42] Y. Hori, R. Takahashi, Y. Yoshinami, A. Murata, *J. Phys. Chem. B* **1997**, *101*, 7075–7081.

[43] M. T. Koper, *Chem. Sci.* **2013**, *4*, 2710.

[44] C.-T. Dinh, T. Burdyny, M. G. Kibria, A. Seifitokaldani, C. M. Gabardo, F. P. García de Arquer, A. Kiani, J. P. Edwards, P. De Luna, O. S. Bushuyev, C. Zou, R. Quintero-Bermudez, Y. Pang, D. Sinton, E. H. Sargent, *Science* **2018**, *360*, 783–787.

[45] E. Pérez-Gallent, M. C. Figueiredo, F. Calle-Vallejo, M. T. Koper, *Angew. Chem. Int. Ed.* **2017**, *56*, 3621–3624.

[46] J. Towns, T. Cockerill, M. Dahan, I. Foster, K. Gaither, A. Grimshaw, V. Hazlewood, S. Lathrop, D. Lifka, G. D. Peterson, R. Roskies, J. R. Scott, N. Wilkins-Diehr, *Comput. Sci. Eng.* **2014**, *16*, 62–74.

TOC

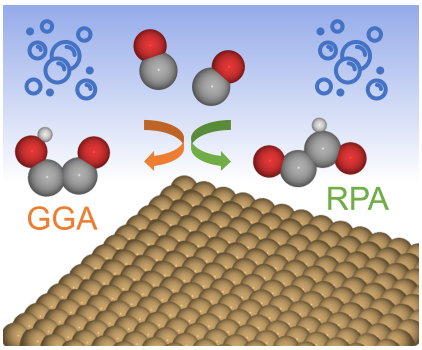

Many-body perturbation theory within its random phase approximation is used to investigate the mechanism of the carbon dioxide reduction reaction on the Cu(100) facet, with special focus on the C-C coupling step. The formation of *OCCHO is proposed as the potential determining step, yielding onset potential and pH dependence matching well with experiments. RPA results also suggest that defective and stepped surfaces may be essential to understand the observed activity of Cu electrocatalysts for C-C bond formation.

keywords: many-body perturbation theory, solvation, CO2 reduction reaction, electrocatalysis